Contents lists available at ScienceDirect

Chemical Engineering Research and Design

journal homepage: www.elsevier.com/locate/cherd

Optimization of Multilayer Standby Mechanisms in Continuous Processes under Varying Loads

*Sing-Zhi Chan, Chuei-Tin Chang**

Department of Chemical Engineering, National Cheng Kung University, Tainan, Taiwan 70101, ROC

ARTICLE INFO

Article history:
Received 11 June 2020
Received in revised form 8 October 2020
Accepted 26 November 2020
Available online 5 December 2020

Keywords:
Standby mechanism
Availability
Expected loss
Genetic Algorithm

ABSTRACT

In modern chemical plants, there is a class of continuous processes operated under varying loads. In these processes, the standby mechanisms are needed to ensure that the downstream demand is always satisfied during the operations. Although a few related studies have been reported in literature, a comprehensive analysis of multilayer standby mechanisms in processes under varying loads has not been carried out. In this paper, a generalized mathematical model is developed to automatically generate the optimal standby mechanisms for any given processes by minimizing the total expected lifecycle expenditure. A Matlab code has been developed to perform these optimization tasks via genetic algorithm. The feasibility and effectiveness of the proposed model are demonstrated with the case study concerning a fan system for providing instrument air in a typical chemical plant. From the optimization results, one can determine the optimum configurations of the standby mechanisms, which include: (1) the number of protection layers, (2) the number of both online and spare sensors in the measurement channels, (3) the corresponding voting-gate logic in each channel, (4) the inspection intervals of switch and (5) the number of spares for switch.

1. Introduction

Standby redundancy is a widely implemented design technique to satisfy the reliability requirements in modern chemical plants. According to Zhang et al. (2006), there are three different types, i.e., *cold*, *hot* and *warm* standbys. The "hot" standbys work in synchrony with the primary online unit(s), while the "cold" standbys are stored offline in shop as spares. The hot standbys are commonly used when the recovery time is of vital importance. In contrast, the cold standbys have their advantages in low energy consumption and low failure rate which are both close to zero. The "warm" standbys are in operation with the online unit but with lighter loads and, thus, can be viewed as the tradeoff between its hot and cold counterparts.

The critical units in a chemical process are often protected with standby mechanisms to ensure that the process is operated properly and continuously over a designated horizon. Chan et al. (2020) have developed a generalized mathematical programming model to generate the optimal designs of multi-layer standby mechanisms in the continuous *steady-state* processes. In that research, the process load is assumed to fluctuate only slightly, while the critical unit may fail after a long period of operation. A different class of processes is considered in the present work. It is assumed that, although the process load may vary significantly and frequently, every critical unit in any such process can be kept at a high level of availability within a relatively short period of time. It is also assumed that, at the end of each operation period, this unit can be brought back to an "as-good-as-new" state via inspections, repairs and/or replacements of its key components.

A standby mechanism is usually facilitated by three types of online components, i.e., the sensing device(s), the switch and the warm standby(s). Based on the assumption that the sensor failures can be detected online, the "corrective" maintenance strategy has often been adopted to repair/replace a sensor as soon as such failure is revealed. Liang and Chang (2008) proposed a spare-supported policy which incorporated the cold standbys of online sensors for improving the overall availability of the measurement systems, while Liao and Chang (2010) extended this policy to the multi-channel monitoring systems. Since the FD failures of switches and warm

* *Corresponding author.*
E-mail address: ctchang@mail.ncku.edu.tw (C.-T. Chang).
https://doi.org/10.1016/j.cherd.2020.11.026

standbys are hidden, the preventive maintenance policies are usually implemented to lower the probabilities of these unobservable events. Specifically, these components should be periodically inspected at designated time intervals and, after inspection, the functional component should be left online while the failed one must be repaired or replaced immediately. Vaurio (1999) incorporated the age-replacement scheme into the preventive maintenance policies to minimize the total cost rate by proper selection of inspection and replacement intervals. Badía et al. (2001) modeled the inspections as imperfect testing in a similar study. Although there are numerous other existing publications related to design and maintenance of standby systems against a constant load, discussions of these studies are omitted in this paper for the sake of conciseness. A more complete literature reviews can be found in Chan et al. (2020).

On the other hand, it should also be noted that there have already been a few published works concerning the standbys against varying loads (Malhotra and Taneja, 2015; Naithani et al., 2017). In these studies, the authors analyzed the standby reliability by using semi-Markov and regenerative point techniques. However, notice that their approach is only suitable for the systems with a small number of standby units. Another approach was developed on the basis of the multivalued decision diagram (MDD). Although it was proposed to evaluate the reliability of the standby mechanisms, this method only focused upon systems with fixed configurations (Amari et al., 2010; Jia et al., 2017).

As mentioned before, the focus of this study is to develop a comprehensive mathematical programming model for synthesizing the optimal designs of multi-layer standby mechanisms in continuous processes under varying loads. For this purpose, the rest of the paper is organized as follows. Section 2 provides a conceptual description of the multilayer standby system structure. Section 3 presents the superstructure of a single protection layer. In Section 4, a generalized event tree is presented for enumerating all scenarios which may induce losses. Section 5 presents the model formulation for characterizing a single protection layer, which consists of the online unit, the monitoring subsystems, the switch and the warm standbys. The governing equations for calculating the total expected lifecycle loss of the multi-layer standby mechanism are provided in Section 6. Section 7 depicts the objective function in the proposed mathematical program, i.e., the total expected lifecycle expenditure, which is the sum of the total expected lifecycle loss, the expected lifecycle costs of monitoring subsystems, the switches and the warm standbys. A case study is presented and discussed in Section 8 to show the feasibility and effectiveness of the proposed method. Conclusions are then given in the final section.

2. Multilayer Standby Mechanisms under Varying Loads

As mentioned before, the standby mechanism under study is used to protect a process against time-variant multi-level loads. Fig. 1shows the mechanism conceptually. In particular, let us assume that this system consists of L identical units, i.e. $P_1, P_2, P_3, \ldots, P_L$, where P_1 serves as the primary online unit while $P_2, P_3, \ldots, P_L$ are the initial warm standbys. Over the entire operation horizon, the chance of failure of any unit is assumed to be negligible. It is also assumed that the process is exposed to a series of increases and/or decreases in loading,

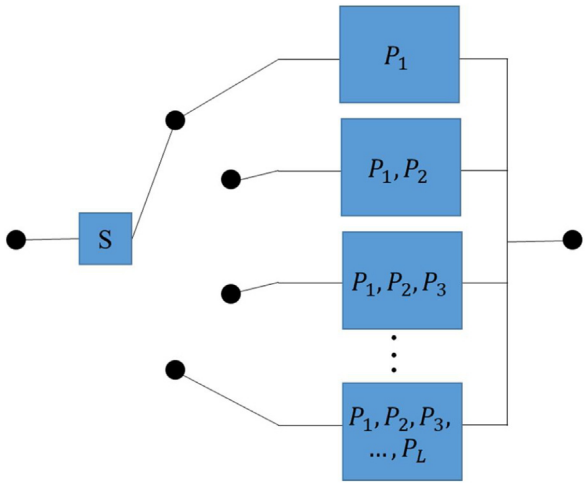

Fig. 1 – Reliability block diagram for multilayer standby mechanisms under varying loads.

and these variations can be monitored with one or more sensors. In response to an initial load increase, the switch (which is denoted as S in Fig. 1) should elevate P_2 to the online state and, thus, P_1 and P_2 could work simultaneously to satisfy the increased demand. If there are further increases in demand at later instances, the switch is supposed to activate the subsequent warm standbys, i.e., $P_3, P_4, P_5, \cdots, P_L$ in sequence. On the other hand, if decreases in process loading are detected, the online units should be deactivated and lowered to the warm standby states one-at-a-time in reverse order. In this research, it is assumed that at least one unit, i.e., P_1, is always kept online over the entire operation horizon. Note that L is referred to as *the number of protection layers* in this paper, while $L-1$ is the maximum number of successive increases/decreases in loading that the standby system can withstand.

It should be noted that the aforementioned standby mechanisms can often be found in modern chemical plants. A typical example is the fan system which provides instrument air to downstream users (Naithani et al., 2017). A second example is the multi-cell cooling tower (Liptak, 1987). Because there may be a change in downstream heat load or ambient wet bulb temperature, it is necessary to manipulate the air flow rate by using different number of cells in the cooling tower to keep the return water temperature within a designated range. The third example is a multi-pump station which transports the specified amount of liquids in plants according to the downstream demand (Liptak, 1987).

3. Superstructure of a Single Protection Layer

To facilitate unambiguous illustration of the above standby mechanisms, let us consider its superstructure in the l^{th} layer (see Fig. 2).

In this structure, ξ_l^p ($l = 1, 2, 3, \ldots, L$ and $p = 1, 2, 3, \ldots$) is a trinary variable which denotes the p^{th} change in process loading over a given time horizon when there is l online units in operation, i.e.

$$\xi_l^p = \begin{cases} -1, \textit{ there is a decrease in process loading} \\ 0, \textit{ there is no change in process loading} \\ +1, \textit{ there is an increase in process loading} \end{cases} \quad (1)$$

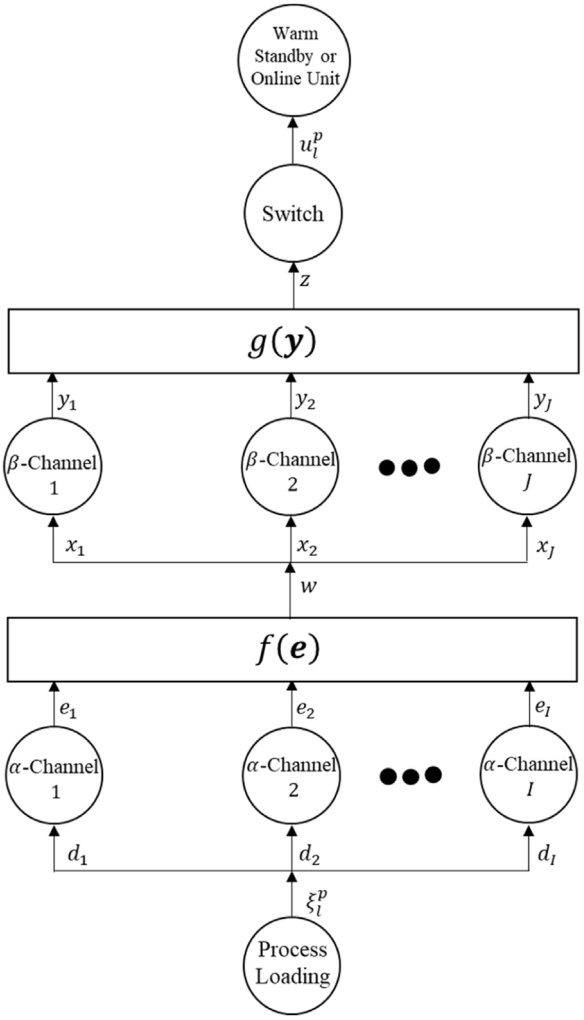

Fig. 2 – Superstructure of the standby mechanism in the l^{th} layer after the p^{th} load change.

A binary variable d_i ($i = 1, 2, \ldots, I$) is then adopted to reflect whether or not the i^{th} process variable (e.g., flowrate, pressure or temperature) varies in response to the above load change, i.e.

$$d_i = \begin{cases} 0, \text{ the } i^{th} \text{ variable does not reveal the change in process loading} \\ 1, \text{ otherwise} \end{cases} \quad (2)$$

One or more identical sensor may be installed to monitor each of the above variables. This collection of identical sensors as a whole is referred to in this paper as an "α -channel" and Fig. 3(a) shows its superstructure. Let us assume that a total of $N_i^{sr\alpha}$ ($N_i^{sr\alpha} \geq 1$) sensors are installed in the i^{th} channel and, in addition, this channel is equipped with a designer-specified $K_i^{sr\alpha}$ -out-of- $N_i^{sr\alpha}$ voting gate to determine whether there is a significant load change. A binary vector $\boldsymbol{e} = \langle e_1, e_2, \ldots, e_I \rangle$ is adopted to characterize all channel outputs, i.e.

$$e_i = \begin{cases} 0, \text{ the } i^{th} \alpha - \text{channel indicates no significant change in process loading} \\ 1, \text{ otherwise} \end{cases} \quad (3)$$

Next, all α -channel outputs are fed into the first so-called "alarm" function $f(\boldsymbol{e})$, i.e.

$$f(\boldsymbol{e}) = \begin{cases} 0, \text{ the alarm of load change is not set off} \\ 1, \text{ otherwise} \end{cases} \quad (4)$$

As a conservative measure, this alarm function is assumed to be fabricated according to the "OR" logic, i.e., the function output w is expressed as:

$$w = f(\boldsymbol{e}) = \begin{cases} 0, \ \forall e_i = 0 \\ 1, \ \exists e_i = 1 \end{cases} \quad (5)$$

The function output w is then fed into a second monitoring subsystem. In a standby mechanism under varying load, the capacity of online unit(s) can usually be adjusted according to demand. This second monitoring subsystem is adopted primarily to detect whether there is a need to increase/decrease an online unit so as to meet the changing demand. For example, the motor speed of online fan(s) should be increased if there is an increase in the downstream air consumption, and an additional fan should be brought online if the demand increase exceeds a threshold value. The flow rate and/or pressure at the common discharge line of all online fans may be measured to determine the air supply capacity. A binary variable x_j ($j = 1, 2, \ldots, J$) is adopted in this work to denote if the j^{th} process variable reaches the threshold level, i.e.

$$x_j = \begin{cases} 0, \text{ the } j^{th} \text{ process variable reveals that the threshold is not reached} \\ 1, \text{ otherwise} \end{cases} \quad (6)$$

The principle of hardware redundancy is again applied to the collection of identical sensors for measuring the same process variable, and these sensors as a whole is referred to as a so-called "β -channel" in this paper. More specifically, a total of $N_j^{sr\beta}$ identical sensors are assumed to be installed in the j^{th} channel and a designer-specified $K_j^{sr\beta}$ -out-of- $N_j^{sr\beta}$ voting gate is implemented to verify whether the threshold capacity of online unit(s) is reached (see Fig. 3(b)). A binary vector $\boldsymbol{y} = \langle y_1, y_2, \ldots, y_J \rangle$ is then used to characterize all outputs of these β -channels, i.e.

$$y_j = \begin{cases} 0, \text{ the } j^{th} \beta - \text{channel indicates the critical capacity of} \\ \quad \text{online unit (s) is not reached} \\ 1, \text{ otherwise} \end{cases} \quad (7)$$

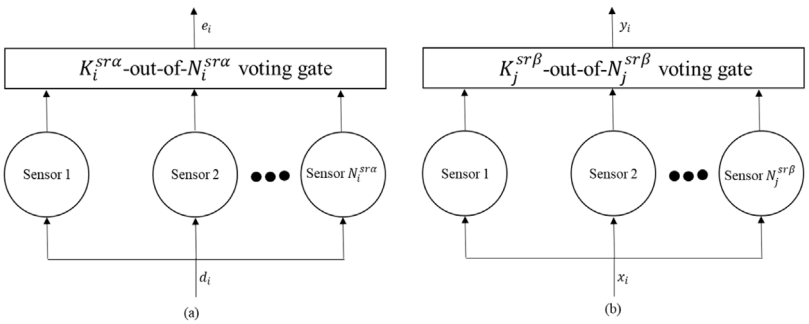

Fig. 3 – Superstructures of (a) α -channel and (b) β -channel.

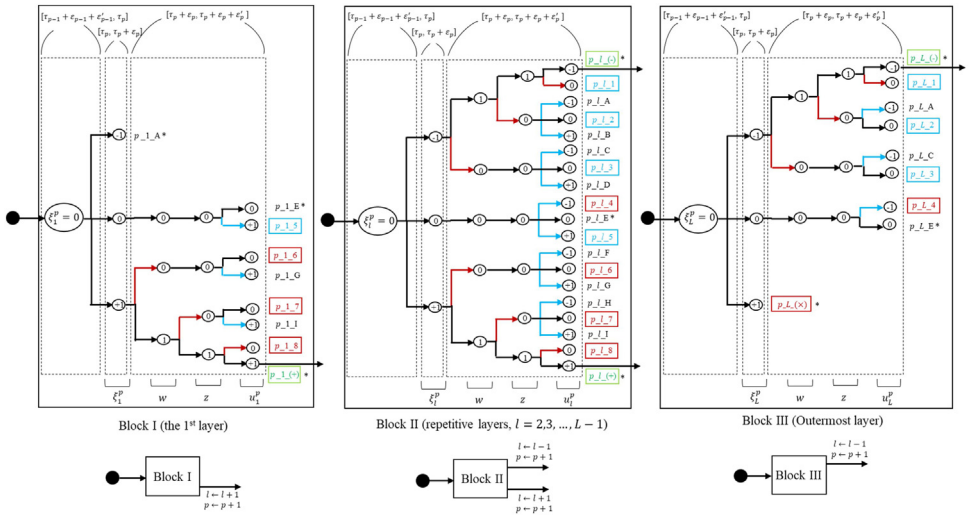

Fig. 4 – Event subtrees for characterizing multilayer standby mechanisms in short-term processes under varying loads.

Next, all β -channel outputs are fed into the second alarm function $g(\mathbf{y})$, i.e.

$$g(\mathbf{y}) = \begin{cases} 0, \text{ the command to add/remove an online unit is not activated} \\ 1, \text{ otherwise} \end{cases} \quad (8)$$

To simplify the model formulation, the "OR" logic is also adopted for this alarm function, i.e., the function output z is expressed as:

$$z = g(\mathbf{y}) = \begin{cases} 0, \ \forall y_j = 0 \\ 1, \ \exists y_j = 1 \end{cases} \quad (9)$$

In other words, a switching action to turn on a warm standby or to deactivate an online unit should be carried out when $z = 1$ (depending on the detected load increase or decrease). Finally, a trinary variable u_l^p is used to represent the switching result in the l^{th} layer after the p^{th} load change, i.e.

$$u_l^p = \begin{cases} -1, \text{ an online unit is switched to warm standby state} \\ 0, \text{ both the online unit and warm standby remain at their original states} \\ +1, \text{ a warm standby is switched to online state} \end{cases} \quad (10)$$

It should be noted that $u_l^p = zw\xi_l^p$ if the standby system behaves normally.

For a multilayer standby mechanisms in short-term processes under varying loads, it should be noted that different layers of protection share the same monitoring subsystems and, also, a single switch is used to execute all switching actions in different protection layers.

4. Generalized Event Tree

Let us first denote the lifecycle of the standby operation to be H (year), where $0 < t \le H$. In this model, H is regarded as a predetermined parameter which equals to the time horizon between two consecutive inspections of the standby system. The inspection intervals of online units and warm standbys are assumed to be short enough so as to ensure high availability.

The three event subtrees in blocks I – III of Fig. 4 and the pseudo flowchart in Fig. 5 can be used to exhaustively enumerate all possible fault propagation scenarios within the standby mechanism over time interval [0, t]. Note that the definitions

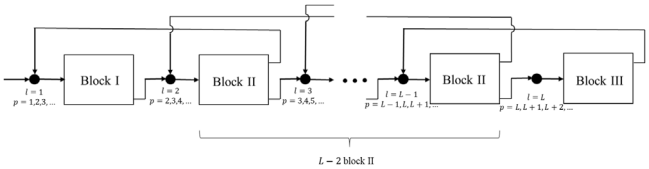

Fig. 5 – Pseudo flowchart for characterizing multilayer standby mechanisms in short-term processes under varying loads.

of ξ_l^p, w, z and u_l^p have already been given in the section 3. In the actual chemical plant, a sensing device may either fail safely (FS) or dangerously (FD). The former failure is neglected in this research because it is usually due to measurement noises which can be eliminated with proper filters. Therefore, the branches directed to $w = 1$ do not emanate from $\xi_l^p = 0$ in the event subtrees. Similarly, the branches ended at $z = 1$ do not come from $w = 0$. Note also that, if a branch goes to $w = 1$ from $\xi_l^p = \pm 1$, each of these two scenarios means that an alarm is set off successfully to announce the corresponding load change. However, if a branch goes to $w = 0$ from $\xi_l^p = +1$ or -1, then every corresponding scenario must be caused by a FD failure of the 1st monitoring subsystem. From $w = 1$, a branch toward $z = 1$ indicates that a mismatch between supply and demand is detected while $z = 0$ implies a FD failure in the 2nd monitoring subsystem.

In the event subtree in block I, it should be noted that the trinary variable $u_1^p \in \{0, +1\}$ only because it is assumed in this study that at least one unit must always be kept online. On the other hand, since the system runs out of warm standbys in the outermost layer (i.e., block III), the trinary variable u_L^p also assume two values only, i.e., $u_L^p \in \{0, -1\}$. In the repetitive layers (i.e., block II) where $l = 2, 3, \ldots, L-1$, two FS switching directions, i.e. $u_l^p = +1$ and $u_l^p = -1$ when $w = 0$, are incorporated in the event tree. On the other hand, when there is a load change and all alarms function properly, all possible scenarios corresponding to FD modes of the switch are grouped in the subtree and denoted as $u_l^p = 0$ because the failure consequences are the same.

In Fig. 4, τ_p is the time when the p^{th} $(p = 1, 2, 3, \cdots, L, \cdots)$ load change takes place and $0 < \tau_1 < \tau_2 < \tau_3 < \cdots < t$. The process loading is assumed to stay constant in time interval $[\tau_{p-1} + \varepsilon_{p-1} + \varepsilon'_{p-1}, \ \tau_p)$. Two additional time intervals, i.e., $\left[\tau_p, \ \ \tau_p + \varepsilon_p \right.$ and $[\tau_p + \varepsilon_p, \ \tau_p + \varepsilon_p + \varepsilon'_p)$, are adopted to represent

the precedence order of the p^{th} change of process loading and the subsequent responses of the monitoring subsystems, the switch and the warm standby (or online unit). Since these events take place almost instantaneously, it is clear that $\varepsilon_p \to 0$ and $\varepsilon_p^{'} \to 0$.

Note that all branches in interval $[\tau_p + \varepsilon_p,\ \tau_p + \varepsilon_p + \varepsilon_p^{'})$ are color coded. The black-colored branches indicate that the corresponding instruments are working normally, while the blue and red branches represent their FS and FD failures respectively. The asterisk-labelled branches are associated with the cases in which the standby mechanisms function properly after the p^{th} change in process loading. Note that scenario p_1_A in block I, which corresponds to the case when a decrease in process loading takes place but the online unit is not switched to the warm standby state, is considered to be normal because of our assumption that at least one online unit is always kept in operation.

To simplify the model formulation, let us assume that the probability of two or more instrument failures occurring within the small time interval $[\tau_p + \varepsilon_p,\ \tau_p + \varepsilon_p + \varepsilon_p^{'})$ is extremely low. Therefore, the corresponding scenarios, i.e., p_l_A, p_l_B, p_l_C, p_l_D, p_l_F, p_l_G, p_l_H and p_l_I, are all ignored in this study. Scenarios p_l_1, p_l_2, p_l_3 and p_l_5 represent the failures of the standby mechanisms result in the supply of the given system to be greater than the demand. On the other hand, scenarios p_l_4, p_l_6, p_l_7 and p_l_8 represent the failures causing the undesirable consequence of demand exceeding supply. Branches $p\_l\_(+)$ s in all subtrees are used to represent the successful activation of warm standby in the l^{th} layer when there is an increase in process loading at τ_p. On the other hand, branches $p\_l\_(-)$ s are used to represent the successful deactivation of an online unit in the l^{th} layer when there is a decrease in process loading at τ_p, and, thus, these branches return to the previous layer (i.e. return to the branches starting with "$\xi_{l-1}^{p+1} = 0$" during a later time interval $[\tau_p + \varepsilon_p + \varepsilon_p^{'}, \tau_{p+1})$. Finally, scenario $p\_l\_(\times)$ in block III is a unique scenario which induces a demand-greater-than-supply outcome although there are no equipment failures. This is due to the fact that the process demand has already been increased for a net total of L times and the given standby mechanism is not equipped to withstand further load increase.

5. Model Formulation for Characterizing a Single Protection Layer

In this section, the mathematical model of every component depicted in the superstructures (see Figs. 2 and 3) is constructed according to the aforementioned event subtrees in Fig. 4.

5.1. *Online units*

Let us assume that, during operations, the online unit(s) experiences a series of load increases and decreases which take place according to two independent homogeneous Poisson processes with intensities λ_+ and λ_- respectively (Kulkarni, 2010). Let us use T_p^+ and T_p^- to denote the inter-arrival times between the p^{th} load increase and decrease and the $p-1^{th}$ load change, respectively, and they should both be random variables that follow distinct exponential distributions. Thus, the probabilities of increase and decrease in process loading during time interval $(\tau_{p-1}, t]$ (denoted as $\Phi_{T_p^+}$ and $\Phi_{T_p^-}$ respectively) can be expressed as follows:

$$\Phi_{T_p^+}(t) = Pr\left\{\left(T_p^+ < t - \tau_{p-1} < T_p^-\right)\right\} = \left[\frac{\lambda_+}{\lambda_+ + \lambda_-}\right]\left[1 - e^{-(\lambda_+ + \lambda_-)(t-\tau_{p-1})}\right] \tag{11}$$

$$\Phi_{T_p^-}(t) = Pr\left\{\left(T_p^- < t - \tau_{p-1} < T_p^+\right)\right\} = \left[\frac{\lambda_-}{\lambda_+ + \lambda_-}\right]\left[1 - e^{-(\lambda_+ + \lambda_-)(t-\tau_{p-1})}\right] \tag{12}$$

The derivations of equations (11) and (12) are provided in part A-1 of the Supplementary Material for the interested readers. On the other hand, the probability of no load changes in time interval $(\tau_{p-1}, t]$ can be expressed as:

$$Pr\left\{\left(T_p^+ > t - \tau_{p-1}\right) \wedge \left(T_p^- > t - \tau_{p-1}\right)\right\} = 1 - \Phi_{T_p^+}(t) - \Phi_{T_p^-}(t) = e^{-(\lambda_+ + \lambda_-)(t-\tau_{p-1})} \tag{13}$$

where, t (year) can be any instance after τ_{p-1} during operation, i.e., $0 < \tau_{p-1} < t \le H$. Let us next consider a particular instance τ_p (year) in interval $(\tau_{p-1}, t]$. The probabilities of load increase and decrease within $(\tau_p,\ \tau_p + d\tau_p]$ can be expressed as the following equations respectively:

$$Pr\left\{\xi_l^p(\tau_p) = +1\right\} = \left.\frac{d\Phi_{T_p^+}(t)}{dt}\right|_{t=\tau_p} d\tau_p = \lambda_+ e^{-(\lambda_+ + \lambda_-)(\tau_p - \tau_{p-1})} d\tau_p \tag{14}$$

$$Pr\left\{\xi_l^p(\tau_p) = -1\right\} = \left.\frac{d\Phi_{T_p^-}(t)}{dt}\right|_{t=\tau_p} d\tau_p = \lambda_- e^{-(\lambda_+ + \lambda_-)(\tau_p - \tau_{p-1})} d\tau_p \tag{15}$$

where $l = 1, 2, 3, \ldots, L$.

5.2. *Monitoring subsystems*

In this study, it is assumed that only the FD failures can take place in the monitoring subsystems. For the first monitoring subsystem which is used to detect the changes in process loading, the conditional probability of FD failure of this subsystem at time τ_p is assumed to be:

$$PFD_{sr\alpha}(\tau_p) = Pr\left\{f(\boldsymbol{e}(\tau_p)) = 0 | \xi_l^p(\tau_p) = +1\right\} = Pr\left\{f(\boldsymbol{e}(\tau_p)) = 0 | \xi_l^p(\tau_p) = -1\right\} \tag{16}$$

By further assuming that the measurement channels yield independent outputs, the conditional FD probability of an OR-logic based monitoring subsystem can be expressed as follows:

$$PFD_{sr\alpha}(\tau_p) = \prod_{i=1}^{I} B_{AL\alpha,i}(\tau_p) \tag{17}$$

where

$$B_{AL\alpha,i}(\tau_p) = Pr\left\{e_i(\tau_p) = 0 | d_i(\tau_p) = 1\right\} \tag{18}$$

For the second monitoring subsystem (which is used to determine if the critical capacity of online unit(s) has been

reached), the corresponding FD conditional probability at time τ_p can be expressed as follows:

$$PFD_{sr\beta}(\tau_p) = Pr\left\{g(\mathbf{y}(\tau_p)) = 0 | w(\tau_p) = 1\right\} \quad (19)$$

For an OR-logic based monitoring subsystem, $PFD_{sr\beta}$ can be further expressed as:

$$PFD_{sr\beta}(\tau_p) = \prod_{j=1}^{J} B_{AL\beta,j}(\tau_p) \quad (20)$$

where

$$B_{AL\beta,j}(\tau_p) = Pr\left\{y_j(\tau_p) = 0 | x_j(\tau_p) = 1\right\} \quad (21)$$

Since each FD sensor failure is considered to be permanent in this study, it is assumed that the spare-supported maintenance policy is adopted to enhance the availability of every measurement channel (Liao and Chang, 2010; Wibisono et al., 2014). Therefore, the *time-dependent* FD conditional probability of the i^{th} α -measurement channel, i.e., $B_{AL\alpha,i}(t)$, and the *time-dependent* FD conditional probability of the j^{th} β -measurement channel, i.e., $B_{AL\beta,j}(t)$, can both be calculated by using the model formulation given in part A-2 of the Supplementary Material.

5.3. *Switch*

Two FS scenarios of the switch can be anticipated, i.e., a unit is switched from online state to warm standby or vice versa when there is no load change. It is assumed in this work that, for the sake of simplicity, their probabilities are the same, i.e.

$$\begin{aligned} PFS_{sw}(\tau_p) &= Pr\left\{u_l^p(\tau_p) = +1 | g(\mathbf{y}_l(\tau_p)) = 0\right\} \\ &= Pr\left\{u_l^p(\tau_p) = -1 | g(\mathbf{y}_l(\tau_p)) = 0\right\} \end{aligned} \quad (22)$$

By assuming that the occurrence time of each FS switching error is uniformly distributed with the same constant density c_{sw}, a *conservative* estimate of $PFS_{sw}(\tau_p)$ can be expressed as:

$$PFS_{sw}(\tau_p) \approx PFS_{sw}(H) = c_{sw}H \quad (23)$$

On the other hand, the FD conditional probability of switch at time τ_l can be written as:

$$PFD_{sw}(\tau_p) = Pr\left\{u_l^p(\tau_p) = 0 | g(\mathbf{y}(\tau_p)) = 1\right\} \quad (24)$$

This *time-dependent* conditional probability can be calculated on the basis of a constant failure rate λ_{sw} (year^{-1}) and the mathematical model of a spare-supported preventive maintenance policy without repairs (see part A-3 of the Supplementary Material).

5.4. *Warm standby*

Since the operating horizon of this standby mechanism is short enough, the probability of online unit failure can be kept at an extremely low level. Since the load of each warm standby is certainly lower than that of an online unit, it is thus assumed that both the FS and FD probabilities of warm standbys are also negligible.

6. Total Expected Lifecycle Loss

The formulas used for determining the expected losses of non-negligible scenarios in the generalized event tree are presented in the sequel. In particular, the calculation procedure of total expected lifecycle loss is divided into two steps for (1) calculating the total expected loss of all scenarios which are labeled according to the convention $l = p$, i.e. scenarios 1_1_5 - 1_1_8, 1_1_(+), l_l_(−), l_l_1 - l_l_8, l_l_(+) (where, $l = 2, 3, \ldots, L-1$), L_L_(−), L_L_1 - L_L_4 and L_L_(×), and (2) estimating the total expected loss of all scenarios which are labeled according to the convention $l < p$, i.e., the scenarios emanated from p_l_(−) ($l = 2, 3, \ldots, L$) in the subtrees in blocks II and III. The total expected losses obtained with these two steps are denoted in this paper as *ExpLoss*1 and *ExpLoss*2 respectively. Thus, the total expected lifecycle loss (IS^H) is:

$$IS^H = ExpLoss1 + ExpLoss2 \quad (25)$$

For the sake of conciseness, only the generalized governing equations for computing the total expected lifecycle loss are given in this section. The detailed derivation of these governing equations of an illustrative 4-layer standby mechanism ($L = 4$) can be found in part A-4 of the Supplementary Material.

Step 1: Calculate *ExpLoss*1 for $l = p$

The *time-dependent* probabilities of scenarios in the event subtrees depicted in Fig. 4 are denoted as $P^{LS}_{p\_l\_(-)}(t)$, $P^{LS}_{p\_l\_1}(t), \cdots, P^{LS}_{p\_l\_8}(t)$, $P^{LS}_{p\_l\_(+)}(t)$ and $P^{LS}_{p\_l\_(\times)}(t)$. To evaluate *ExpLoss*1, the ordinary differential equations (ODEs) listed below in equations (26) – (37) and the ODEs in parts A-2 and A-3 in Supplementary Material should be solved simultaneously to obtain the time-dependent probabilities of all repetitive scenarios, i.e.

$$\begin{aligned} &\mathbf{Scenario\ l\_(-)}: \xi_1^l(\tau_1) \\ &= -1, w(\tau_1) = 1, z(\tau_1) = 1, u_1^l(\tau_1) = -1 (l = 2, 3, \ldots, L) \end{aligned}$$

$$\begin{aligned} \frac{dP^{LS}_{l\_l\_(-)}(t)}{dt} &= [\lambda_- e^{-(\lambda_+ + \lambda_-)t}][1 - PFD_{sr\alpha}(t)] \\ &[1 - PFD_{sr\beta}(t)][1 - PFD_{sw}(t)] P^*_{l-1}(t) \end{aligned} \quad (26)$$

$$\begin{aligned} &\mathbf{Scenario\ l\_1}: \xi_1^l(\tau_1) = -1, w(\tau_1) \\ &= 1, z(\tau_1) = 1, u_1^l(\tau_1) = 0 (l = 2, 3, \ldots, L) \end{aligned}$$

$$\begin{aligned} \frac{dP^{LS}_{l\_l\_1}(t)}{dt} &= [\lambda_- e^{-(\lambda_+ + \lambda_-)t}][1 - PFD_{sr\alpha}(t)] \\ &[1 - PFD_{sr\beta}(t)][PFD_{sw}(t)] P^*_{l-1}(t) \end{aligned} \quad (27)$$

$$\begin{aligned} &\mathbf{Scenario\ l\_2}: \xi_1^l(\tau_1) = -1, w(\tau_1) \\ &= 1, z(\tau_1) = 0, u_1^l(\tau_1) = 0 (l = 2, 3, \ldots, L) \end{aligned}$$

$$\frac{dP_{l\_l\_2}^{LS}(t)}{dt}=\begin{cases}\left[\lambda_{-}e^{-(\lambda_{+}+\lambda_{-})t}\right][1-PFD_{sr\alpha}(t)] \\ [PFD_{sr\beta}(t)][1-2\times PFS_{sw}(t)]P_{l-1}^{*}(t),\ l<L \\ \left[\lambda_{-}e^{-(\lambda_{+}+\lambda_{-})t}\right][1-PFD_{sr\alpha}(t)][PFD_{sr\beta}(t)] \\ [1-PFS_{sw}(t)]P_{l-1}^{*}(t),\ l=L\end{cases} \tag{28}$$

$$\textbf{Scenario}\_l\_\textbf{3}:\xi_1^l(\tau_l)=-1,\mathrm{w}(\tau_l)=0,\mathrm{z}(\tau_l)=0,\mathrm{u}_1^l(\tau_l)=0(l=2,3,\ldots,\mathrm{L}.)$$

$$\frac{dP_{l\_l\_3}^{LS}(t)}{dt}=\begin{cases}\left[\lambda_{-}e^{-(\lambda_{+}+\lambda_{-})t}\right][PFD_{sr\alpha}(t)][1-2\times PFS_{sw}(t)]P_{l-1}^{*}(t),\ l<L \\ \left[\lambda_{-}e^{-(\lambda_{+}+\lambda_{-})t}\right][PFD_{sr\alpha}(t)][1-PFS_{sw}(t)]P_{l-1}^{*}(t),\ l=L\end{cases} \tag{29}$$

$$\textbf{Scenario}\_l\_\textbf{4}:\xi_1^l(\tau_l)=0,\mathrm{w}(\tau_l)=0,\mathrm{z}(\tau_l)=0,(l=2,3,\ldots,\mathrm{L})$$

$$\frac{dP_{l\_l\_4}^{LS}(t)}{dt}=[e^{-(\lambda_{+}+\lambda_{-})t}][c_{sw}]P_{l-1}^{*}(t) \tag{30}$$

$$\textbf{Scenario}\_l\_\textbf{5}:\xi_1^l(\tau_l)=0,\mathrm{w}(\tau_l)=0,\mathrm{z}(\tau_l)=0,\mathrm{u}_1^l(\tau_l)=+1(l=1,2,\ldots,\mathrm{L}-1)$$

$$\frac{dP_{l\_l\_5}^{LS}(t)}{dt}=[e^{-(\lambda_{+}+\lambda_{-})t}][c_{sw}]P_{l-1}^{*}(t) \tag{31}$$

$$\textbf{Scenario}\_l\_\textbf{6}:\xi_1^l(\tau_l)=+1,\mathrm{w}(\tau_l)=0,\mathrm{z}(\tau_l)=0,\mathrm{u}_1^l(\tau_l)=0(l=1,2,\ldots,\mathrm{L}-1)$$

$$\frac{dP_{l\_l\_6}^{LS}(t)}{dt}=\begin{cases}\left[\lambda_{+}e^{-(\lambda_{+}+\lambda_{-})t}\right][PFD_{sr\alpha}(t)][1-PFS_{sw}(t)]P_{l-1}^{*}(t),\ l=1 \\ \left[\lambda_{+}e^{-(\lambda_{+}+\lambda_{-})t}\right][PFD_{sr\alpha}(t)][1-2\times PFS_{sw}(t)]P_{l-1}^{*}(t),\ l>1\end{cases} \tag{32}$$

$$\textbf{Scenario}\_l\_\textbf{7}:\xi_1^l(\tau_l)=+1,\mathrm{w}(\tau_l)=1,\mathrm{z}(\tau_l)=0,\mathrm{u}_1^l(\tau_l)=0(l=1,2,\ldots,\mathrm{L}-1)$$

$$\frac{dP_{l\_l\_7}^{LS}(t)}{dt}=\begin{cases}\left[\lambda_{+}e^{-(\lambda_{+}+\lambda_{-})t}\right][1-PFD_{sr\alpha}(t)] \\ [PFD_{sr\beta}(t)][1-PFS_{sw}(t)]P_{l-1}^{*}(t),\ l=1 \\ \left[\lambda_{+}e^{-(\lambda_{+}+\lambda_{-})t}\right][1-PFD_{sr\alpha}(t)][PFD_{sr\beta}(t)] \\ [1-2\times PFS_{sw}(t)]P_{l-1}^{*}(t),\ l>1\end{cases} \tag{33}$$

$$\textbf{Scenario}\_l\_\textbf{8}:\xi_1^l(\tau_l)=+1,\mathrm{w}(\tau_l)=1,\mathrm{z}(\tau_l)=1,\mathrm{u}_1^l(\tau_l)=0(l=1,2,\ldots,\mathrm{L}-1)$$

$$\frac{dP_{l\_l\_8}^{LS}(t)}{dt}=[\lambda_{+}e^{-(\lambda_{+}+\lambda_{-})t}][1-PFD_{sr\alpha}(t)][1-PFD_{sr\beta}(t)][PFD_{sw}(t)]P_{l-1}^{*}(t) \tag{34}$$

$$\textbf{Scenario}\_l\_(+):\xi_1^l(\tau_l)=+1,\mathrm{w}(\tau_l)=1,\mathrm{z}(\tau_l)=1,\mathrm{u}_1^l(\tau_l)=+1(l=1,2,\ldots,\mathrm{L}-1)$$

$$\frac{dP_{l\_l\_(+)}^{LS}(t)}{dt}=[\lambda_{+}e^{-(\lambda_{+}+\lambda_{-})t}][1-PFD_{sr\alpha}(t)][1-PFD_{sr\beta}(t)][1-PFD_{sw}(t)]P_{l-1}^{*}(t) \tag{35}$$

$$\textbf{Scenario}L\_L\_(\times):\xi_{\mathrm{L}}(\tau_{\mathrm{L}})=+1$$

$$\frac{dP_{L\_L\_(\times)}^{LS}(t)}{dt}=[\lambda_{+}e^{-(\lambda_{+}+\lambda_{-})t}]P_{L-1}^{*}(t) \tag{36}$$

Note that the connective terms used in the aforementioned ODEs should be computed as follows:

$$\frac{dP_{l}^{*}(t)}{dt}=[\lambda_{+}][1-PFD_{sr\alpha}(t)][1-PFD_{sr\beta}(t)][1-PFD_{sw}(t)]P_{l-1}^{*}(t) \tag{37}$$

where $l=1,2,\ldots,L-1$. Note also that $P_0^*(t)=1$.

If the lifecycle is H year ($H<1$), one can determine *ExpLoss*1 according to the following formula:

$$\begin{aligned}ExpLoss1=C_a\int_0^H&\Big[P_{1\_1\_5}^{LS}+P_{L\_L\_1}^{LS}+P_{L\_L\_2}^{LS}+P_{L\_L\_3}^{LS}\\&+\sum_{l=2}^{L-1}\left(P_{l\_l\_1}^{LS}+P_{l\_l\_2}^{LS}+P_{l\_l\_3}^{LS}+P_{l\_l\_5}^{LS}\right)\Big]dt\\+C_b\int_0^H&\left[\begin{array}{l}P_{1\_1\_6}^{LS}+P_{1\_1\_7}^{LS}++P_{1\_1\_8}^{LS}+P_{L\_L\_4}^{LS}+P_{L\_L\_(\times)}^{LS}\\+\sum_{l=2}^{L-1}\left(P_{l\_l\_4}^{LS}+P_{l\_l\_6}^{LS}+P_{l\_l\_7}^{LS}+P_{l\_l\_8}^{LS}\right)\end{array}\right]dt\end{aligned} \tag{38}$$

where C_a and C_b are the expected losses of a supply-greater-than-demand scenario and a demand-greater-than-supply scenario respectively.

Step 2: Estimate *ExpLoss*2 for $l<p$

Since the scenarios corresponding to $l<p$ are associated with all branches emanated from nodes $p\_l\_(-)$ ($l=2,3,\ldots,L$), *ExpLoss*2 can be estimated as follows:

$$ExpLoss2=\sum_{l=2}^{L}EqPr_l\times Loss_l \tag{39}$$

where $Loss_l$ is the sum of all expected losses for $l = p$ incurred in the last $L - l + 2$ blocks in the pseudo flowchart (see Fig. 5 and part A-4 of the Supplementary Material for detailed derivation and calculation procedure), while $EqPr_l$ is the equivalent probability of all possible routes that induce $Loss_l$. The latter can be calculated as follows:

$$EqPr_l = \begin{cases} \sum_{r_l=1}^{R_l} \left(\frac{PI^{LS}_{l\_l\_0}}{PI^{LS}_{(l-2)\_(l-2)\_9}}\right)^{r_l} \text{ when } l = L \\ \sum_{r_l=1}^{R_l} \left(\frac{PI^{LS}_{l\_l\_0}}{PI^{LS}_{(l-2)\_(l-2)\_9}}\right)^{r_l} + \sum_{s_{l+1}=1}^{R_{l+1}} \left(\frac{PI^{LS}_{(l+1)\_(l+1)\_0}}{PI^{LS}_{(l-1)\_(l-1)\_9}}\right)^{s_{l+1}} \left(\frac{PI^{LS}_{l\_l\_0}}{PI^{LS}_{(l-2)\_(l-2)\_9}}\right) \text{ when } l = L-1 \\ \sum_{r_l=1}^{R_l} \left(\frac{PI^{LS}_{l\_l\_0}}{PI^{LS}_{(l-2)\_(l-2)\_9}}\right)^{r_l} + \sum_{r_{l+1}=0}^{R_{l+1}-1R_{l+1}-r_{l+1}} \sum_{s_{l+1}=1} \left(\frac{PI^{LS}_{(l+2)\_(l+2)\_0}}{PI^{LS}_{l_9}}\right)^{r_{l+1}} \left(\frac{PI^{LS}_{(l+1)\_(l+1)\_0}}{PI^{LS}_{(l-1)\_(l-1)\_9}}\right)^{s_{l+1}} \left(\frac{PI^{LS}_{l\_l\_0}}{PI^{LS}_{(l-2)\_(l-2)\_9}}\right) \text{ when } l = 2, 3, \ldots, L-2 \end{cases} \quad (40)$$

Note that the symbol $PI^{LS}_{scenario}$ in the above equation is adopted to represent the integral of $P^{LS}_{scenario}(t)$ over the entire horizon of lifecycle, i.e.

$$PI^{LS}_{scenario} = \int_0^H P^{LS}_{scenario}(t)\, dt \quad (41)$$

Note also that R_l ($l = 2, 3, \ldots, L$) in equation (40) is the total number of repeated emanation times from scenarios $l\_l\_(-)$ until $PI^{LS}_{p\_l\_(-)}$ ($p = l+2, l+4, l+6, \ldots$) is lower than a user-defined small positive number.

7. Objective Function

The objective function to be minimized in the proposed programming model is the total expected lifecycle expenditure, which includes the total expected lifecycle loss (IS^H), the expected lifecycle cost of monitoring subsystems (LCC^{sr}), the expected lifecycle cost of switches (LCC^{sw}) and the expected lifecycle cost of standby subsystem (LCC^{wb}), i.e.

$$obj = IS^H + LCC^{sr} + LCC^{sw} + LCC^{wb} \quad (42)$$

If there is a budget limit (PC_{ibc}), an additional constraint can be imposed as follow:

$$PCT^{sr} + PCT^{sw} + PCT^{wb} \le PC_{ibc} \quad (43)$$

where PCT^{sr}, PCT^{sw} and PCT^{wb} are the total purchase costs of the monitoring subsystems, switches and standby subsystem respectively.

7.1. Expected lifecycle cost of monitoring subsystems

The total expected lifecycle cost of the two monitoring subsystems (which include all α - and β - channels) can be further classified into three types, i.e., the total purchase cost (PCT^{sr}), the total expected repair cost ($RrCT^{sr}$) and the total expected replacement cost ($RplCT^{sr}$). Specifically, the total expected lifecycle cost of the two monitoring subsystems can be expressed as:

$$LCC^{sr} = PCT^{sr} + RrCT^{sr} + RplCT^{sr} \quad (44)$$

For the sake of conciseness, the calculation steps of PCT^{sr}, $RrCT^{sr}$ and $RplCT^{sr}$ are not described in details here. One can refer to part A-2 in the Supplementary Material for further explanations.

7.2. Expected lifecycle cost of switches

The expected lifecycle cost (LCC^{sw}) of switches is the sum of the total purchase cost (PCT^{sw}) and the total inspection cost ($InspCT^{sw}$) of switches. In other words, the lifecycle cost of switches can be expressed as follow:

$$LCC^{sw} = PCT^{sw} + InspCT^{sw} \quad (45)$$

One can refer to part A-3 in the Supplementary Material for further illustration on computation methods of PCT^{sw} and $InspCT^{sw}$.

7.3. Lifecycle cost of standby subsystem

The lifecycle cost of standby subsystem (LCC^{wb}) is the total purchase cost of warm standbys (PCT^{wb}) only. For a standby subsystem with L protection layers, the lifecycle cost can be expressed as:

$$LCC^{wb} = PCT^{wb} = L \times PC^{wb} \quad (46)$$

where PC^{wb} is the purchase cost of a single standby unit.

8. Case Study

The feasibility and effectiveness of the proposed design method are demonstrated in this section with a case study. Fig. 6 shows a typical fan system for providing instrument air in a process plant (Liptak, 1987). Fan #1 is always running in the entire time horizon under consideration while the others are the warm standbys. When the supply of instrument air is greater than the process demand, the consequence is an unnecessary waste of electricity. On the other hand, there should be safety and/or operational problems if the downstream demand is greater than supply. After executing a comprehensive hazard assessment, C_a and C_b are chosen to be 0 and 10^6 USD respectively. These selections imply that the expected loss of any supply-greater-than-demand event is negligible when compared to that of a demand-greater-than-supply case. It is assumed in this example that the operational horizon of the fan system is 4 months, i.e., $H = 4/12$ (year).

In the following case study, a flowrate channel (which is referred to as a α -channel in this study) is assumed to be available in the first monitoring subsystem to reveal the changes in process loading. To determine the capacity of online fan(s), the flow rate and pressure at the common discharge side of

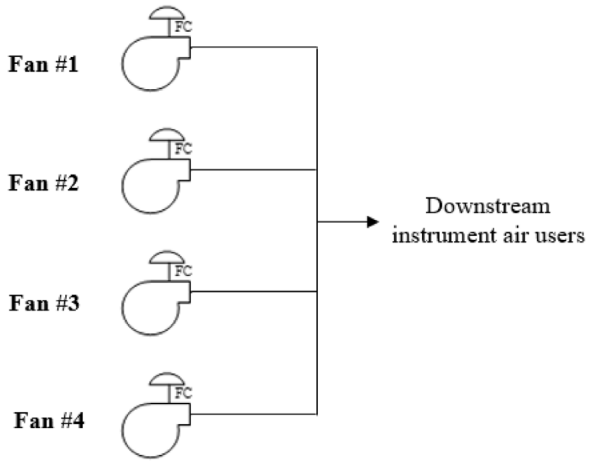

Fig. 6 – Fan system for instrument air ($L = 4$).

Table 1 – Specifications of sensors.

	Pressure	Flow rate
FD failure rate (year^{-1})	1.41	2.4
Repair rate (year^{-1})	100	50
Replacement rate (year^{-1})	365	365
Purchase cost (USD)	350	90
Repair cost(USD)	25	15
Replacement cost (USD)	15	10

Table 2 – Specifications of switches.

FD failure rate (year^{-1})	0.22
Purchase cost (USD)	100
Inspection cost (USD)	10
FS failure probability of a single switch	0.2

all online fans are measured. In other words, the flowrate and pressure sensors are adopted as the β -channels in the second monitoring subsystem. The specifications of sensors and switches are listed in Tables 1 and 2 respectively. On the other hand, the purchase cost of a standby unit is assumed to be 2000 USD.

In this work, the maximum numbers of online and spare sensors are both set to be 3 for each channel. In addition, the maximum length of inspection intervals for a switch is set to be 2 months. Moreover, the maximum allowable number of protection layers is assumed to be six, i.e. $L \leq 6$.

The numerical optimization runs were carried out with the genetic algorithm (GA) (Michalewicz, 1996) in Matlab R2018b environment on an Intel Core i7 3.60 GHz PC. This Matlab code, which can be found in Supplementary Material, can also be developed for any other standby applications according to the generalized model presented in this paper and a user-specified maximum allowable layer number. The parameter settings and convergence behaviors of GA in the case study are described in part A-5 of the Supplementary Material. Table 3 summarizes the optimization results for standby mechanisms with different initial budget constraints when $\lambda_+ = \lambda_- = 5$ (year^{-1}), while Table 4 summarizes the optimization results for standby mechanisms with different shock intensity when there are no initial budget constraints. The corresponding optimal configurations can be found in part A-6 in Supplementary Material. Figs. 7 and 8 show the expected loss of each scenario. For the sake of conciseness, scenarios $l\_l\_(-)$ ($l = 2, 3, \ldots, L$) in these figures actually represent all loss-induced scenarios emanated from branches $l\_l\_(-)$. For comparison purpose, the sum of the expected losses in every layer is also presented on the top of the Figs. 7 and 8.

From the aforementioned optimization results, several interesting features can be observed:

a) From Table 3, one can observe that the objective value (i.e. total expected lifecycle expenditure) of the standby mechanism increases as the initial budget tightens. A lower initial budget certainly results in a standby mechanism with fewer layers. Although a reduction in the layer number causes a decrease in purchase cost, the total expected lifecycle loss should increase significantly and, as a result, the objective value must still increase.
b) In cases when there is no budget constraint (Table 4), the optimal number of warm standbys (protection layers) does not always reach the upper bound, i.e., six, adopted in all optimization runs.
c) From Fig. 7, it can be observed that the total expected loss of the scenarios corresponding to the outermost layer, e.g., scenario $L\_L\_(\times)$, can be reduced by installing an extra layer of protection. For example, the expected loss of scenario $2\_2\_(\times)$ in Run # D (i.e., 37806 USD) can be reduced to 13786 USD (total expected loss of 3rd layer in Run # C) by increas-

Table 3 – Optimization results for standby mechanisms corresponding to $\lambda_+ = \lambda_- = 5$ (year^{-1}).

Run #	A	B	C	D
Initial budget (USD)	None	10000	8000	6000
Total expected lifecycle expenditure (USD)	21073	21858	28445	51987
Purchase cost (USD)	11350	9350	7350	5350
Maintenance cost (USD)	91	91	91	91
Total expected lifecycle loss (USD)	9632	12417	21004	46547
Number of layers in standby mechanism	5	4	3	2

Table 4 – Optimization results for standby mechanisms with different shock intensity.

Run #	A	E	F	G
λ_+, λ_- $\left(year^{-1}\right)$	5.0	3.5	2.0	0.5
Total expected lifecycle expenditure (USD)	21073	18562	14945	8523
Purchase cost (USD)	11350	9350	7350	5350
Maintenance cost (USD)	91	91	91	91
Total expected lifecycle loss (USD)	9632	9122	7504	3082
Layer of standby mechanism	5	4	3	2

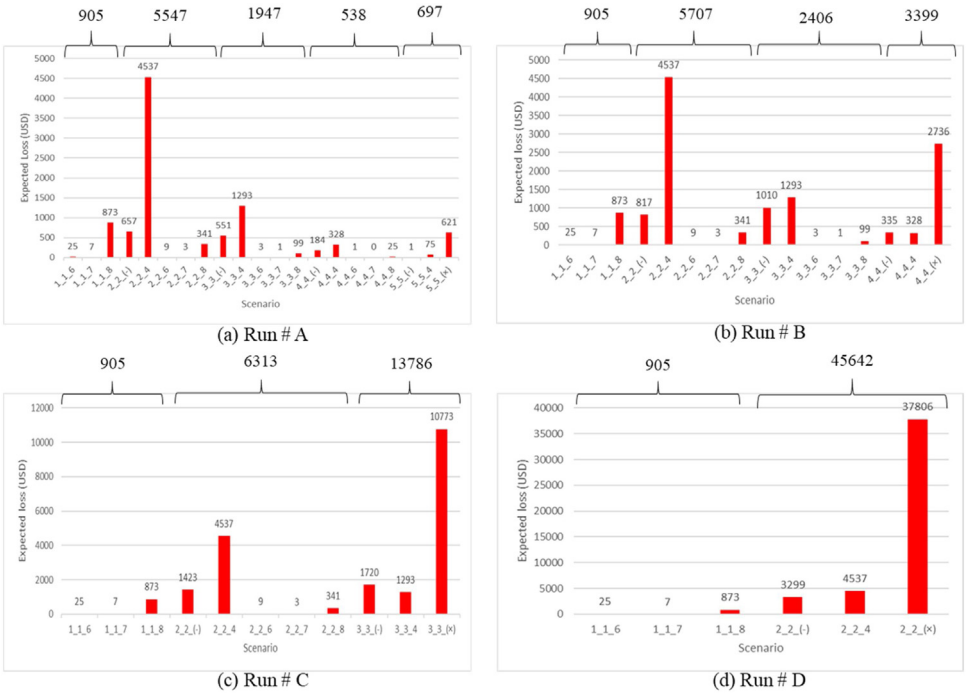

Fig. 7 – Expected losses of different scenarios ($\lambda_+ = \lambda_- = 5$ year^{-1}).

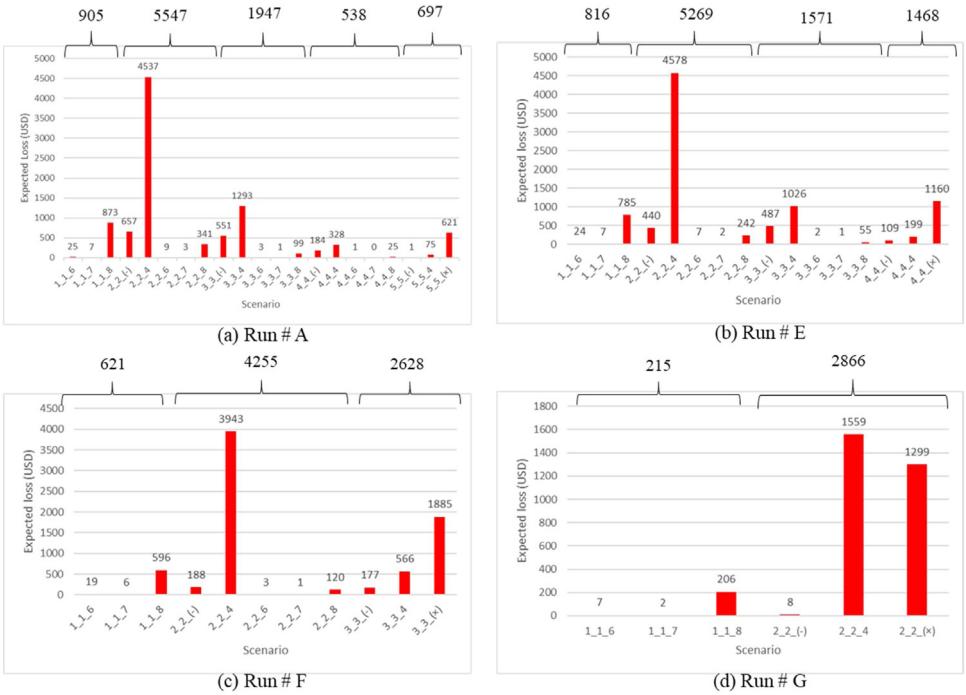

Fig. 8 – Expected losses of different scenarios (different shock intensity).

ing the number of protection layers from 2 to 3. Similarly, the expected loss of scenario 3_3_(×) in Run # C (i.e., 10773 USD) can be lowered to 3399 USD (total expected loss of 4th layer in Run # B) by increasing the number of protection layers from 3 to 4.

d) Shock intensities can be used to characterize the rates of demand changes. A high shock intensity value implies that the mean inter-arrival time is short. From Table 4, one can observe that the objective value is increased if the shock intensities are raised to higher levels when there is no initial budget limit. This is due to the fact that higher shock intensities result in more frequent demand changes. As a result, the probabilities of loss-induced scenarios should be increased and hence the total expected lifecycle loss increased also. Consequently, the standby mechanism is usually equipped with multiple layers to protect the given process.

e) From Figs. 7 and 8, one can see that scenarios l_l_4 ($l = 2, 3, \ldots, L$) and $L\_L\_(\times)$ are the major contributors to the expected lifecycle loss. The former scenarios are concerned with the FS mode of switch which changes the online unit of the l^{th} layer to the warm standby state. In these cases, there could be subsequent safety and/or operational problems because the need for instrument air is not satisfied. Note that the high expected losses of these scenarios are primarily due to the relatively high FS probability of switch.

On the other hand, scenario $L\_L\_(\times)$ is associated with the case in which the air supply of the entire system is insufficient after L successive increases in process loading. In this case, the high expected loss can in general be lowered by installing one more protection layer.

9. Conclusions

In this research, a generalized mathematical programming model and the corresponding Matlab code have been developed to automatically generate the optimal designs of multilayer standby mechanisms in the continuous processes under varying loads. By slightly modifying the GA code, one can apply this model to a wide variety of other industrial and commercial problems of the same nature without ad-hoc approach. The feasibility and effectiveness of the proposed model (and code) are demonstrated with a case study, i.e., the fan system for providing instrument air in a typical chemical plant (Liptak, 1987). One can determine the optimal configurations of the standby mechanisms under different initial budget constraints or different shock intensities.

It should be noted that the proposed standby mechanism is only suitable for the process in which the load may vary frequently and the risk of critical unit failure is relatively low in the operating horizon. A future study will be performed to address the issues concerning the more general standby mechanisms in which the critical unit failures and demand fluctuations are both present.

Declaration of interests

The authors declare that they have no known competing financial interests or personal relationships that could have appeared to influence the work reported in this paper.

Acknowledgement

This work is supported by the ministry of science and technology of the Taiwan government under grant 108-2221-E-006-149-.

Appendix A. Supplementary data

Supplementary material related to this article can be found, in the online version, at doi:https://doi.org/10.1016/j.cherd.2020.11.026.

References

Amari, S.V., Xing, L., Shrestha, A., Akers, J., Trivedi, K.S., 2010. Performability analysis of multistate computing systems using multivalued decision diagrams. IEEE Trans. Comput. 59, 1419–1433, http://dx.doi.org/10.1109/TC.2009.184.

Badía, F.G., Berrade, M.D., Campos, C.A., 2001. Optimization of inspection intervals based on cost. J. Appl. Probab. 38, 872–881, http://dx.doi.org/10.1239/jap/1011994178.

Chan, S.Z., Liu, H.Y., Luo, Y.K., Chang, C.T., 2020. Optimization of Multilayer Standby Mechanisms in Continuous Chemical Processes. Ind. Eng. Chem. Res. 59 (5), 2049–2059, http://dx.doi.org/10.1021/acs.iecr.0c00233.

Jia, H., Ding, Y., Peng, R., Song, Y., 2017. Reliability Evaluation for Demand-Based Warm Standby Systems Considering Degradation Process. IEEE Trans. Reliab. 66, 795–805.

Kulkarni, V.G., 2010. Modeling and Analysis of Stochastic Systems, Second Edi. ed. Taylor & Francis Books, New York, NY.

Liang, K.H., Chang, C.T., 2008. A simultaneous optimization approach to generate design specifications and maintenance policies for the multilayer protective systems in chemical processes. Ind. Eng. Chem. Res. 47, 5543–5555, http://dx.doi.org/10.1021/ie071188z.

Liao, Y.C., Chang, C.T., 2010. Design and maintenance of multichannel protective systems. Ind. Eng. Chem. Res. 49, 11421–11433, http://dx.doi.org/10.1021/ie901818e.

Liptak, B., 1987. Optimization of unit operations. Chilton Book Company, Radnor, PA.

Malhotra, R., Taneja, G., 2015. Stochastic Analysis of a Two-Unit Cold Standby System Wherein Both Units May Become Operative Depending upon the Demand. J. Qual. Reliab. Eng., http://dx.doi.org/10.1155/2014/896379.

Michalewicz, Z., 1996. Genetic Algorithms + Data Structures = Evolution Programs, Third, Rev. ed. Springer-Verlag Berlin Heidelberg, New York, NY.

Naithani, A., Parashar, B., Bhatia, P.K., Taneja, G., 2017. Probabilistic analysis of a 3-unit induced draft fan system with one warm standby with priority to repair of the unit in working state. Int. J. Syst. Assur. Eng. Manag. 8, 1383–1391, http://dx.doi.org/10.1007/s13198-017-0608-6.

Vaurio, J.K., 1999. Availability and cost functions for periodically inspected preventively maintained units. Reliab. Eng. Syst. Saf. 63, 133–140, http://dx.doi.org/10.1016/S0951-8320(98)00030-1.

Wibisono, E., Adi, V.S.K., Chang, C.T., 2014. Model based approach to identify optimal system structures and maintenance policies for safety interlocks with time-varying failure rates. Ind. Eng. Chem. Res. 53, 4398–4412, http://dx.doi.org/10.1021/ie402902q.

Zhang, T., Xie, M., Horigome, M., 2006. Availability and reliability of k-out-of-(M+N):G warm standby systems. Reliab. Eng. Syst. Saf. 91, 381–387, http://dx.doi.org/10.1016/j.ress.2005.02.003.